

Model-free readout-error mitigation for quantum expectation values

Ewout van den Berg, Zlatko K. Mineev, and Kristan Temme

IBM Quantum, T.J. Watson Research Center

Yorktown Heights, NY, USA

(Dated: January 28, 2022)

Measurements on current quantum processors are subject to hardware imperfections that lead to readout errors. These errors manifest themselves as a bias in quantum expectation values. Here, we propose a very simple method that forces the bias in the expectation value to appear as a multiplicative factor that can be measured directly and removed at the cost of an increase in the sampling complexity for the observable. The method assumes no specific form of the noise, but only requires that the noise is ‘weak’ to avoid excessive sampling overhead. We provide bounds relating the error in the expectation value to the sample complexity.

I. INTRODUCTION

Quantum algorithms [1–8] for near-term devices can often be described by the execution of a reasonably-shallow quantum circuit followed by the measurement of an observable through sampling. A general assumption for near-term devices is that proper quantum error-correction [9–12] is not yet available. As a result, noise parameters, such as coherence time, dictate the maximum depth of a circuit and therefore determine the size of the calculation that can be performed. Even when working within these limitations, hardware noise can still affect expectation values in the form of a bias. Error-mitigation techniques have therefore been introduced to remove this bias and produce more accurate expectation values. These techniques come at the additional cost of repeating the computation, possibly with altered parameters, increased sampling cost, or additional classical post processing. For the mitigation of errors that occur during the application of the quantum circuit, several schemes have been proposed [13–21] and implemented experimentally [22, 23].

In this work, we consider the mitigation of readout errors that occur during the final measurement step of the computation. We focus on the computation of the expectation values of Pauli observables. Since Pauli matrices constitute a Hermitian matrix basis, they can represent any observable [24]. Moreover, any observable that can be expanded in a polynomial number of Pauli matrices, such as local Hamiltonians, can be estimated efficiently by measuring the expectation values of Pauli observables, due to linearity of the expectation value.

After a quantum circuit has been applied, we can measure a Pauli observable. This is done by rotation of the observable to the computational basis using single-qubit Clifford gates, followed by measurement in this basis and some basic classical post processing. In the absence of readout errors, the measurement output of n qubits is fully described by a probability distribution p over the 2^n computational basis states. The standard model for readout errors is given by a classical noise map A [25–27], which maps the noise-free p to the noisy \tilde{p} readout distribution by $\tilde{p} = Ap$. The readout map A is a 2^n -by-

2^n left-stochastic matrix, where the entry $A_{i,j}$ denotes the probability of measuring the i -th instead of the j -th computational basis state, for $i, j \in \{0, 1\}^n$.

A direct approach to mitigate the effect of read-out errors has frequently been to estimate columns of A by measuring the output frequencies \hat{r}_x for different bit strings x and then to apply the matrix A^{-1} for mitigation [3, 26, 28]. Explicit representation and inversion of A is of course feasible only when the system size is small, or when the noise can be assumed to factorize such that noise on individual or small groups of qubits can be modeled and inverted independently. However, experiments have shown that the noise tends to be correlated [29], which invalidates the use of product approximations to the stochastic matrix. Several approaches have been proposed to deal with this more difficult scenario [30–32] as well as with other settings [32–34]. Recently, a readout error-mitigation scheme for correlated noise with a formal performance guarantee on sampling overhead depending on the noise strength was proposed and implemented experimentally in [35]. In this approach, the noise map does not need to be explicitly inverted and the model can be concisely represented using $\mathcal{O}(\text{poly}(n))$ parameters.

Here, we propose a readout-error mitigation method that is motivated by work on quantum benchmarking protocols [36, 37]. The method, introduced in Section II, randomizes the output channel by uniformly applying random Pauli bit flips prior to measurement, which are tracked and used in the subsequent analysis. In Section III we show that this randomization transforms the action of an arbitrary noise map A into a single multiplicative factor per Pauli observable; that is, it diagonalizes the measurement channel. The multiplicative factors can be measured directly, in the absence of the quantum circuit. By dividing out this factor, the bias-free mitigated Pauli expectation value is obtained. The method does not require a model of the physical measurement noise and does not make assumptions on the noise strength. In fact, the method only makes the assumption that the circuit can be initialized in the zero state.

The shot-noise variance of the mitigated estimate scales inversely proportional with the magnitude of noise factor. In Section IV, we show how this magnitude de-



FIG. 1. Illustration of the (a) measurement and (b) calibration circuits used for the estimation of error-mitigated averages.

depends on the underlying noise strength and analyze the required number of measurement samples to attain a desired estimation accuracy. Simulations in Section V indicate that the method scales reasonably to larger system sizes in the presence of moderate noise.

II. METHOD

Consider a system of n qubits and order the set of Pauli operators such that P_q denotes a unique Pauli operator indexed by $q \in \mathcal{P} := [0, 4^n - 1]$. The Pauli-Z operators are assigned indices $\mathcal{Z} := [0, 2^n - 1]$ and the set of indices corresponding to Pauli-X operators is denoted \mathcal{X} . Given $r, s \in \mathbb{Z}_2^n$ with inner product $\langle r, s \rangle = \sum_i r_i s_i$, we define $Z^s = \bigotimes_{i=1}^n \sigma_z^{s_i}$ and likewise for X_s with σ_z replaced by σ_x . Interpreting s as an integer index, we set $P_s = Z^s$.

Starting from the initial state

$$\rho_0 = |0\rangle\langle 0| = 2^{-n}(I + \sigma_z)^{\otimes n} = 2^{-n} \sum_{j \in \mathcal{Z}} P_j, \quad (1)$$

we want to estimate the Pauli-Z component P_i in state $\rho = U\rho_0 U^\dagger$ obtained by applying operator U , namely

$$\langle P_i \rangle_\rho = \text{Tr}(P_i \rho). \quad (2)$$

We assume that the initial state is ρ_0 and that all measurements are performed in the computational basis. This means that we can only evaluate (2) for $i \in \text{Pauli-Z}$. Expectation values for other Paulis can be obtained by incorporating an appropriate basis change in operator U .

In order to estimate (2) we run various instances of the circuit given in Figure 1(a). The circuit is parameterized by Pauli index q , and unitary C (or the circuit that implements it). Choosing C to be the identity results in a simplified circuit, as shown in Figure 1(b). The Pauli index q will be sampled from some index set \mathcal{S} to be specified later. The protocol to acquiring measurement outcomes for N circuit instances is given by:

Protocol AcquireData(\mathcal{S}, C, N)

- 1: Initialize an empty data set \mathcal{D}
- 2: **for** $i = 1, \dots, N$ **do**
- 3: Uniformly sample q from index set \mathcal{S}
- 4: Execute the circuit in Figure 1(a) with Pauli P_q and unitary C
- 5: Record the measurement outcome x and add tuple (q, x) to \mathcal{D}
- 6: **return** \mathcal{D}

Each measurement outcome is represented by an element $x \in \mathbb{Z}_2^n$. In classical post-processing of the acquired data, we use the function

$$f(\mathcal{D}, s) = \frac{1}{|\mathcal{D}|} \sum_{(q,x) \in \mathcal{D}} \gamma_{s,q} (-1)^{\langle s,x \rangle}, \quad (3)$$

where $\gamma_{a,b}$ has the value 1 if Paulis P_a and P_b commute and the value -1 otherwise (these sign changes with respect can be omitted if we flip measurement bits according to the sampled q value). The protocol for estimating $\langle Z^s \rho \rangle$ is then as follows:

Protocol 1

1. $\mathcal{D}_0 = \text{AcquireData}(\mathcal{X}, I, N)$
2. $\mathcal{D}_1 = \text{AcquireData}(\mathcal{X}, U, N)$
3. Return estimate $f(\mathcal{D}_1, s)/f(\mathcal{D}_0, s)$

Note that the data acquired in steps 1 and 2 can be reused to evaluate the quantity in step 3 for different values of s . Moreover, the data from step 1 is independent of U and can therefore be used in error mitigation of measurement of other states as well. For simplicity we set the number of samples in each of the two data sets to N . More generally we could choose different numbers of samples for each of these steps.

III. DERIVATION

Ideal measurements in the computational basis can be written in terms of positive operator-valued measures $E_x = |x\rangle\langle x|$ for $x \in \mathbb{Z}_2^n$. We assume that measurements are affected by a noise map A , such that measurement y can be misinterpreted as x with probability $A_{x,y} = \langle x|A|y\rangle$. Using this, we can define noisy measures $\tilde{E}_x = \sum_y A_{x,y} |y\rangle\langle y|$. Now, for $s \in \mathbb{Z}_2^n$, define

$$X_s := \sum_a |a+s\rangle\langle a| = \sum_a |a\rangle\langle a+s| = X_s^\dagger, \text{ and}$$

$$Z_s := \sum_a (-1)^{\langle s,a \rangle} |a\rangle\langle a|.$$

We would like to estimate the expectation value

$$\langle Z_w \rangle_\rho = \text{Tr}(Z_w \rho) = \sum_{x \in \mathbb{Z}_2^n} (-1)^{\langle w,x \rangle} \text{Tr}(E_x \rho). \quad (4)$$

Substituting E_x by \tilde{E}_x gives an unmitigated noisy estimate $\langle \tilde{Z}_s \rangle_\rho$. In order to mitigate the readout error, our algorithm applies a random bit flips prior to measurement, and then either applies the same bit flips directly after the (noisy) measurement, or equivalently adjust signs in the estimation of the expectation value. The random bit flip, obtained by applying X_s for a randomly sampled s , can be applied before the noisy measurement, or directly after an ideal measurement but just prior to

the noise map A . Using the latter view, we can define the twirled noise map A^* as

$$\begin{aligned} A^* &:= \frac{1}{2^n} \sum_s X_s A X_s^\dagger = \frac{1}{2^n} \sum_s \sum_{a,b} A_{a,b} X_s |a\rangle \langle b| X_s^\dagger \\ &= \frac{1}{2^n} \sum_s \sum_{a,b} A_{a,b} |a+s\rangle \langle b+s|, \end{aligned}$$

with associated measure $\tilde{E}_x^* = \sum_y A_{x,y}^* |y\rangle \langle y|$. Substitution in (4) then gives us the twirled noisy expectation

$$\begin{aligned} \langle \tilde{Z}_w^* \rangle_\rho &:= \sum_{x \in \mathbb{Z}_2^n} (-1)^{\langle w, x \rangle} \text{Tr}(\tilde{E}_x^* \rho) \\ &= \sum_{x,y} (-1)^{\langle w, x \rangle} \langle x | A^* | y \rangle \text{Tr}(|y\rangle \langle y| \rho) \end{aligned} \quad (5)$$

In order to simplify this, first define

$$|v_w\rangle = \sum_x (-1)^{\langle w, x \rangle} |x\rangle.$$

We then have

$$\begin{aligned} A^* |v_w\rangle &= \frac{1}{2^n} \sum_{s,x} \sum_{a,b} (-1)^{\langle w, x \rangle} A_{a,b} |a+s\rangle \langle b+s|x\rangle \\ &\stackrel{(s=b+x)}{=} \frac{1}{2^n} \sum_x \sum_{a,b} (-1)^{\langle w, x \rangle} A_{a,b} |a+b+x\rangle \\ &= \frac{1}{2^n} \sum_x \sum_{a,b} (-1)^{\langle w, x+a+b \rangle} A_{a,b} |x\rangle \\ &= \lambda_w |v_w\rangle, \text{ with } \lambda_w = \frac{1}{2^n} \sum_{a,b} (-1)^{w \cdot (a+b)} A_{a,b}. \end{aligned}$$

In other words, $|v_w\rangle$ is an (unnormalized) eigenvector of A^* with corresponding eigenvalue λ_w . We therefore have $\langle v_w | A^* = \lambda_w \langle v_w |$, and it immediately follows that we can rewrite (5) as

$$\begin{aligned} \langle \tilde{Z}_w^* \rangle_\rho &= \langle v_w | A^* \sum_y |y\rangle \text{Tr}(|y\rangle \langle y| \rho) \\ &= \lambda_w \langle v_w | \sum_y |y\rangle \text{Tr}(|y\rangle \langle y| \rho) \\ &= \lambda_w \sum_{x,y} (-1)^{\langle w, x \rangle} \langle x | y \rangle \text{Tr}(|y\rangle \langle y| \rho) \\ &= \lambda_w \sum_x (-1)^{\langle w, x \rangle} \text{Tr}(|x\rangle \langle x| \rho) \\ &= \lambda_w \langle Z_w \rangle_\rho. \end{aligned}$$

For the initial state $\rho = |0\rangle \langle 0|$ we have $\langle Z_w \rangle_\rho = 1$ and therefore $\langle \tilde{Z}_w^* \rangle_\rho = \lambda_w$. The protocol estimates this quantity, and then uses it to obtain noise-mitigated estimates $\langle Z_w \rangle_\rho$ for other values of ρ .

A. Alternative derivation

As an alternative derivation, consider the super-operator representation of the state in the Pauli basis as $|\rho\rangle\rangle$. In the case of ideal measurements in the computational basis, the readout probabilities are given by projection operator $[H_n^{-1}, 0]$ with $H_n = H^{\otimes n}$, where H the unnormalized Hadamard matrix $X + Z$. The noisy readout probabilities are then given by the vector

$$A [H_n^{-1}, 0] |\rho\rangle\rangle.$$

Conversion of binary measurements to Pauli-Z observables is done through the Walsh-Hadamard transformation. By appropriately ordering the Pauli-Z operators, this amounts to multiplication by H_n . The vector of Pauli-Z observable expectation values is then given by

$$H_n A [H_n^{-1}, 0] |\rho\rangle\rangle = [H_n A H_n^{-1}, 0] |\rho\rangle\rangle = [M, 0] |\rho\rangle\rangle$$

with $M = H_n A H_n^{-1}$. For the proposed error-mitigation scheme we add a random Pauli-X operator P_q prior to measurement and appropriate sign changes to the estimate. The effect of this is multiplication with diagonal matrices D_q and D'_q with diagonal elements $\gamma_{v,q} = (-1)^{\langle v, q \rangle}$ for v in \mathcal{Z} and $\mathcal{P} \setminus \mathcal{Z}$, respectively:

$$D_q [M, 0] \begin{bmatrix} D_q & 0 \\ 0 & D'_q \end{bmatrix} |\rho\rangle\rangle = [D_q M D_q, 0] |\rho\rangle\rangle$$

Multiplication from the left and right by a diagonal matrix $\text{diag}(d_q)$ amounts to elementwise multiplication with matrix $d_q d_q^T$. The expectation of these matrices over the Pauli-X group satisfies $\mathbb{E}_{q \in \mathcal{X}} [d_q d_q^T] = I$. The expected observable vector is therefore given by

$$[M \odot I, 0] |\rho\rangle\rangle.$$

We can determine $\lambda = \text{diag}(M)$ by multiplying with $|\rho_0\rangle\rangle$, which is a vector whose first 2^n elements are one and all remaining elements are zero. Once we know λ we can easily divide it out to obtain unbiased Pauli-Z estimates.

IV. ANALYSIS

A. Sample complexity

Protocol 1 estimates $\langle \tilde{Z}^s \rangle_\rho$ as $f(\mathcal{D}_1, s)/f(\mathcal{D}_0, s)$, which is of the form \hat{x}/\hat{y} . We now consider the sample complexity of the protocol: what value of N we should choose, such that with probability at least $1 - \delta$ the final estimate deviates at most ϵ from the exact value? Before doing so, we first consider the accuracy of the estimate in the case we can estimate x and y up to an additive error of at most α .

Lemma IV.1. *Let x, y be such that $0 \leq |x| \leq |y| \leq 1$. Given estimates \hat{x}, \hat{y} with $|x - \hat{x}| \leq \alpha$ and $|y - \hat{y}| \leq \alpha$, such that $0 \leq \alpha \leq |y|/2$. Then*

$$\left| \frac{\hat{x}}{\hat{y}} - \frac{x}{y} \right| \leq \frac{4\alpha}{y}.$$

Proof. Assume without loss of generality that $x, y \geq 0$. Taking the Taylor-series expansion around zero for sufficiently small α we have in the worst case that

$$\begin{aligned} \frac{\hat{x}}{\hat{y}} &= \frac{x + \alpha}{y - \alpha} = \frac{x}{y} + \left(1 + \frac{x}{y}\right) \sum_{k=1}^{\infty} \left(\frac{\alpha}{y}\right)^k \\ &\leq \frac{x}{y} + \left(1 + \frac{x}{y}\right) \cdot \left(\frac{1}{1 - \alpha/y} - 1\right) \\ &\leq \frac{x}{y} + \left(1 + \frac{x}{y}\right) \cdot \left(\frac{\alpha/y}{1 - \alpha/y}\right) \leq \frac{x}{y} + \frac{4\alpha}{y}. \end{aligned}$$

In the last inequality we use the fact that $x/y \leq 1$, and $1 - \alpha/y \geq 1/2$. A lower bound can be derived similarly to obtain the given result. \square

With this we can obtain the following sample complexity:

Theorem IV.2. *With probability at least $1 - \delta$, protocol 1 estimates (2) with error at most ϵ for a fixed $i \in \mathcal{Z}$ when the number of samples N satisfies*

$$N \geq \frac{32 \log(4/\delta)}{M_{i,i}^2 \epsilon^2}.$$

Proof. Protocol 1 acquires data and estimate different quantities using the function in (3). For a fixed i and j , we can view each term in the summation as an independent ± 1 sample from a certain distribution depending on U that marginalizes over Pauli indices p and q . For the error in the estimated quantities, we therefore apply Hoeffding's inequality, which states that, given independent random variables X_i from any distribution over $[-1, 1]$, the deviation of $\bar{X} = N^{-1} \sum_{i=1}^N X_i$ to the expected value $\mathbb{E}(X)$ satisfies

$$\Pr\left(\left|\bar{X} - \mathbb{E}(X)\right| \geq \alpha\right) \leq 2 \exp\left(-\frac{1}{2} N \alpha^2\right). \quad (6)$$

We want to ensure that probability of deviating from the expectation by α or more, is bounded by $\delta/2$. Using the union bound it then follows that the numerator and denominator are α close to their expectation with probability at least $1 - \delta$. Bounding the failure probability in (6) from above by $\delta/2$ gives the sufficient condition

$$N \geq \frac{2 \log(4/\delta)}{\alpha^2}. \quad (7)$$

We now need to choose α such that the final estimate is ϵ accurate. From Lemma IV.1 we see that it suffices to take $4\alpha/y \leq \epsilon$, where $y = f_I(i) = M_{i,i}$. Substituting $\alpha = \epsilon M_{i,i}/4$ in (7) then gives the desired result. \square

As discussed in more detail in Section IV C, the term $M_{i,i}$ is expected to scale weakly exponential in the weight of the Pauli-Z observable with a base that deviates from unity by the magnitude of the noise. The increase in sampling complexity therefore depends on the strength of the noise similar to the quasi-probabilistic noise cancellation method in ref. [13].

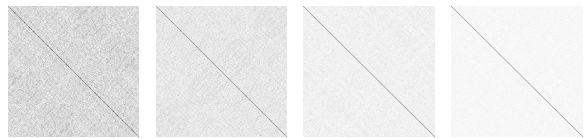


FIG. 2. Diagonalization masks for 12 qubits, obtained by averaging the outer products of commutation vectors d_q using, from left to right, 30, 100, 1000, and 3000 random $q \in \mathcal{X}$.

B. Number of circuit instances

For a given q , the term $D_q M D_q$ can be written as the elementwise product of M and the outer product $d_q d_q^T$. The outer product has the important property that diagonal elements are always one, irrespective of the signs in d_q . For randomly sampled $q \in \mathcal{X}$ or $q \in \mathcal{P}$, each off-diagonal value has an equal chance of being plus or minus one, and therefore has an expected value of zero. When the number of qubits n is small we can iterate over all possible q values and obtain exact diagonalization of M . For larger values of n this becomes intractable and we can therefore only approximately diagonalize M , as illustrated in Figure 2. For calibration we estimate $e_i M \mathbf{1} = M_{i,i} + e_i M (\mathbf{1} - e_i)$. In order to suppress the second term we need to sample sufficiently many circuits instances. For the actual estimate of $M_{i,i}$ itself we simply need to sample sufficiently many times regardless of the circuit instance. At this point we should also remark that the actual procedure depends on measurements from the probability vector $\tilde{p} = A[H^{-1}, 0] D_q |\rho_0\rangle\rangle$ and we therefore need to sample each circuit sufficiently many times.

In this section we give bounds on the number of circuit instances we need to estimate $M_{i,i}$ to a given accuracy. Given that we multiply by an approximately diagonal mask, this bound depends in part on the maximum off-diagonal elements in M . We show how this corresponds to properties of the transfer matrix A and study these properties for different types of transfer matrices. Our final estimates are given by the ratio of two quantities and we therefore consider how the estimation error in these quantities affect the result. Note that through this section we work with the full matrix representation for clarity; as shown in Section II, processing itself is done based on individual elements.

For the the number of circuit instances we need to approximately diagonalize M , we have the following result:

Theorem IV.3. *Given k randomly sampled values $q_1, \dots, q_k \in \mathcal{X}$ and an index set $\mathcal{I} \subseteq [2^n]$. Define*

$$\hat{M} = \frac{1}{k} \sum_{\ell=1}^k (D_{q_\ell} M D_{q_\ell}) \quad \text{and} \quad \beta = \max_{i \in \mathcal{I}} \sum_{j \neq i} |M_{i,j}|.$$

Then we satisfy $|e_i \hat{M} (\mathbf{1} - e_i)| \leq \epsilon$ and $|\hat{M}_{i,i} - M_{i,i}| \leq \epsilon$ simultaneously for all $i \in \mathcal{I}$ with probability at least $1 - \delta$

whenever

$$k \geq 2 \frac{\log(2/\delta) + n \log(2) + \log(|\mathcal{I}|)}{\epsilon^2/(1+\beta)^2}. \quad (8)$$

Proof. Let i be any element in \mathcal{I} . For scaling of the off-diagonal elements we uniformly sample X from $\{-1, 1\}$. If we can ensure that each element is scaled by a factor at most ϵ_b , then we have an additive term with magnitude at most $\epsilon_b \beta$ in the estimation of $M_{i,i}$. For the estimation of $M_{i,i}$ itself, we apply (6) with X following an appropriate distribution on $[-1, 1]$ and a maximum deviation of ϵ_a . Using a union bound over the off-diagonal elements in the row we obtain the condition

$$2 \exp(-\frac{1}{2}k\epsilon_a^2) + 2(2^n - 1) \exp(-\frac{1}{2}k\epsilon_b^2) \leq \delta \quad (9)$$

In case $\beta = 0$ we can choose $\epsilon_a = \epsilon$ and let $\epsilon_b \rightarrow \infty$. Using a union bound over the rows in \mathcal{I} gives a sufficient number of circuit instances of

$$k \geq \frac{\log(2/\delta) + \log(|\mathcal{I}|)}{\epsilon^2/2}.$$

For the more general case where $\beta \neq 0$ we choose $\epsilon_a = \epsilon_b$, which reduces condition (9) to

$$2^n \exp(-\frac{1}{2}k\epsilon_a^2) = \exp(n \log(2) - \frac{1}{2}k\epsilon_a^2) \leq \delta/2. \quad (10)$$

In order to satisfy $\epsilon_a + \epsilon_b \beta \leq \epsilon$ we must choose $\epsilon_a \leq \epsilon/(1+\beta)$. Combined with a union bound, obtained by multiplying the left-hand side of (9) by the cardinality of \mathcal{I} , this gives the sample complexity stated in 8. \square

As an aside, we note that diagonalization of quantum noise channels using Pauli twirls follows exactly the same principle as the one we use for diagonalizing M . A simple modification of Theorem IV.3 can then be used to determine the number of circuits needed to ensure that all off-diagonal noise terms are bounded by ϵ .

C. Example transition matrices

For a given transition matrix A we define a corresponding transformed matrix $M = HAH^{-1}$. This can be seen as readout transition matrix for Pauli-Z operators. It is easily seen that $M^{-1} = HA^{-1}H^{-1}$ whenever the inverse of A exists. For convex combinations of two error channels, namely $A = \mu A_1 + (1-\mu)A_2$ with $\mu \in [0, 1]$, we have $M = \mu M_1 + (1-\mu)M_2$. This straightforwardly generalizes to the convex combination of any number of transition matrices.

As a simple example of a transition matrix, consider the case where the outcome of each qubit is independently flipped with some probability r . The transition matrix for a single qubit is then given by

$$A_i = \begin{pmatrix} 1-r_i & s_i \\ r_i & 1-s_i \end{pmatrix}, \quad (11)$$

with $r = s$. These matrices are then combined into a global transition matrix $A = A_{s_1} \otimes \cdots \otimes A_{s_n}$. The corresponding Pauli readout transition matrix then has a particularly simple structure:

$$HAH^{-1} = \bigotimes_{\ell=1}^n (H_2 A_{r_\ell} H_2^{-1}) = \bigotimes_{\ell=1}^n \begin{bmatrix} 1 & 0 \\ 0 & (1-2r_\ell) \end{bmatrix} \quad (12)$$

In this case, since M is already diagonal, we do not need to shrink the off-diagonal elements. It therefore suffices to choose an arbitrary but fixed value for $q \in \mathcal{X}$ for the circuits, rather than sample it. Choosing $q = 0$ simplifies the resulting circuits. Assume for simplicity that all probabilities r_ℓ are equal to r , then it follows from (12) that the diagonal element $M_{i,i}$ is directly related to the weight of the Pauli-Z operator P_i . For each σ_z term in P_i we have a multiplicative term $(1-2r)$. The diagonal term for P_i with k non-identity term is then given by $(1-2r)^k$. The term $(1-2r)^k$ is bounded below by $1-2kr$, that means that for 30 qubits with 1% probability of a measurement flip, the diagonal elements in M are still at least 0.4. In the noiseless case the bit flip probability is zero and we obtain $A = M = I$.

The transition matrix for the case where we only measure zeros is given by $A = e_0 e^T$ with a corresponding matrix $M = e e_0^T$. In case each outcome is measured with equal probability, regardless of the state, we have $A = 2^{-n} e e^T$ and $M = e_0 e_0^T$. Although not realistic by themselves, these matrices could be used in convex combinations with other transition matrices. A good, but not very realistic, example of a transition matrix that is perfectly invertible but provides difficulty for our method is the following permutation matrix:

$$A = \begin{bmatrix} \cdot & \cdot & 1 & \cdot \\ 1 & \cdot & \cdot & \cdot \\ \cdot & \cdot & \cdot & 1 \\ \cdot & 1 & \cdot & \cdot \end{bmatrix}, \quad HAH^{-1} = \begin{bmatrix} 1 & \cdot & \cdot & \cdot \\ \cdot & \cdot & -1 & \cdot \\ \cdot & 1 & \cdot & \cdot \\ \cdot & \cdot & \cdot & -1 \end{bmatrix}$$

If we have access to an approximate inverse \hat{A}^{-1} , we can adjust our scheme to work with $D_q H \hat{A}^{-1} \tilde{p}$ instead of $D_q H \tilde{p}$. This form of preconditioning could help increase the magnitude of the diagonal elements in M or reduce that of the off-diagonal elements but may be computationally expensive.

D. Practical considerations

In most of the discussion so far we have assumed ideal state preparation. Suppose that, instead of $\rho_0 = |0\rangle\langle 0|$, we can only prepare $\hat{\rho}_0$. For calibration this means that, after diagonalization of M , we obtain the vector

$$(M \odot I)Z(\hat{\rho}_0) = \text{diag}(Z(\hat{\rho}_0))m \quad (13)$$

rather than m . If we assume that state preparation for qubits is independent and that each qubit ℓ is initialized

to state $(1-\alpha_\ell)|0\rangle\langle 0|+\alpha|1\rangle\langle 1| = \frac{1}{2}(I+(1-2\alpha_\ell)\sigma_z)$, then we have

$$Z(\hat{\rho}_0)^T = \bigotimes_{\ell} \begin{pmatrix} 1 \\ 1-2\alpha_\ell \end{pmatrix}.$$

Under this assumption, that means that, if we can estimate the α_ℓ values, we can incorporate this information in (13) to better estimate m .

Once the calibration data set has been acquired it can be used to mitigate readout errors for circuits with various U , possibly with basis changes. In practical systems we can expect gradual changes in systemic gate and readout errors. That means that calibration data has a limited lifetime. For error mitigation in the proposed approach we traverse the calibration data whenever we want to compute the correction factor for an individual Pauli-Z operator. This approach makes updates to the calibration data set very light weight: we could simply augment the calibration data with time stamps and periodically add some new data points while retiring data that falls outside the current time window. For approaches based on explicit inversion of the transfer matrix, any such update would amount to regeneration of the entire matrix and its inverse. The computation complexity for updating the correction factor using (3) is linear in the size of the data set. The evaluation of an element in the Hadamard matrix and commutation between two n -qubit Pauli operators both take $\mathcal{O}(n)$ time.

Note that the scalar terms $H_{m,i}$ in (3) could be replaced by elements from any other matrix, say G with $|G_{m,i}| \leq 1$, provided that the (relevant) diagonal elements of GAH^{-1} are sufficiently large.

As mentioned in Section IV, we can only access information about M by sampling from $\tilde{p} = AH^{-1}D_qZ(\rho_0)$ for each instance q . In practice we therefore need to make a tradeoff between the number of circuit instances and the number of samples per circuit. We leave a detailed analysis of this for future work.

V. SIMULATION

We evaluate the performance of the proposed method on a simple quantum circuit consisting of a single $R_y(\alpha_i\theta)$ gate on each qubit, where α_i is a scaling parameter that differs for each qubit, and θ is a global phase. We choose $\alpha_1 = 3$ and $\alpha_i = 0.15$ for all remaining qubits. The Pauli transfer matrix for $R_y(\theta) = \exp(-i\theta Y/2)$ is given by

$$T_{R_y(\theta)} = \begin{pmatrix} 1 & 0 & 0 & 0 \\ 0 & \cos(\theta) & 0 & -\sin(\theta) \\ 0 & 0 & 1 & 0 \\ 0 & \sin(\theta) & 0 & \cos(\theta) \end{pmatrix}.$$

When applied to a Pauli-Z operator with σ_z components for qubits $i \in \mathcal{I}$, the final weight is given by

$$\prod_{i \in \mathcal{I}} \cos(\alpha_i\theta) \quad (14)$$

We simulate noisy readout by forming transition matrix A with individual asymmetric bit-flip channels with a larger weight for 1 to 0 transitions. The transition matrix additionally includes correlated readout errors on pairs of qubits. In Figures 3(a)–(c) we illustrate a seven-qubit transition matrix A , the corresponding $M = HAH^{-1}$, as well as the product $A_s^{-1}A$, where A_s is the transition matrix that we would obtain if we would determine the exact bit-flip frequencies for each of the qubits, and form the corresponding transition matrix. The diagonal terms of the aforementioned three matrices, along with the sum of absolute values of the off-diagonal elements in M , are plotted in Figure 3(d).

As a first experiment we consider a 12-qubit system. For the proposed method we sample 256 circuits each with 512 measurements. For matrix inversion we take the same total number of measurements, but spread out over each of the 2,048 columns, each corresponding to a unique circuit, thus giving a maximum of 64 measurements per circuit. The resulting estimates for the weights of Pauli-Z operators with σ_z at the first qubit, respectively all qubits are shown in Figures 4(a) and 4(b) for a range of θ values in (14). The estimates obtained using the proposed approach are very close to the exact solution; so close in fact that the curves are hard to distinguish. Given that the transition matrix contains correlated noise terms, the exact bit-flip approximation can never exactly mitigate the readout noise, as seen from the rather poor performance. Finally, the results based on the inverse of the estimated transition matrix \hat{A} appear to be biased in both settings and relatively lead more accurate, but still nowhere near the performance of the proposed method. By increasing the number of samples per circuit we can improve the accuracy of the estimates, as illustrated in Figure 4(c) and 4(d). However, even with 32 times more measurements, the results obtained using matrix inversion are still not as accurate as those obtained using the proposed method. Note that the estimation error for the low-weight Pauli operator in Figure 4(d) is much lower than the weight- n Pauli.

In the next set of experiments we fix the number of circuits for the proposed method to 512 and vary the number of measurements per circuit instance. We sort the resulting estimation errors in magnitude for the different θ values and plot the result in Figure 4(e). We compare the results with those obtained using the matrix-inversion approach, and display the equivalent number of measurements per circuits. Forming the full matrix requires $2^{12} = 2,048$ circuits, which means that the actual number of measurements per circuit is four times lower than the number shown. To match the performance of the proposed method with 32 samples per circuit, the matrix-inversion approach requires an equivalent of 8,192 samples per circuit, which is 128 times more measurements in total. Similarly, In Figure 4(f) we compare the performance of the methods by fixing the number of circuits to 32 and varying the number of measurements per circuit.

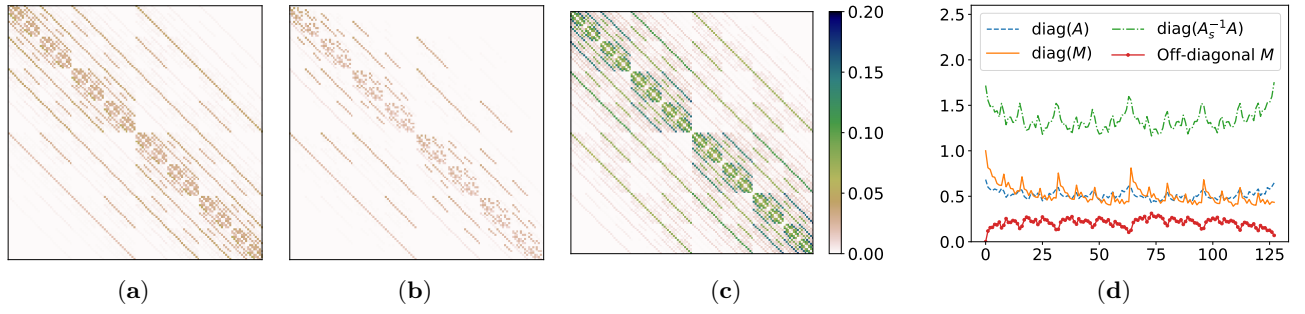


FIG. 3. Magnitude of the off-diagonal matrix entries of (a) transition matrix A , (b) matrix $M = HAH^{-1}$, and (c) matrix $A_s^{-1}A$, where A_s is the single-qubit bit-flip model of A . We zero out the diagonal elements to highlight the off-diagonal structure and relative magnitude of the elements; the diagonal matrix elements are shown in plot (d) along with the sum of absolute values of the off-diagonal elements in M . If the transition matrix A did not include any correlated readout errors, the matrix $A_s^{-1}A$ would be the identity matrix with unit diagonal entries.

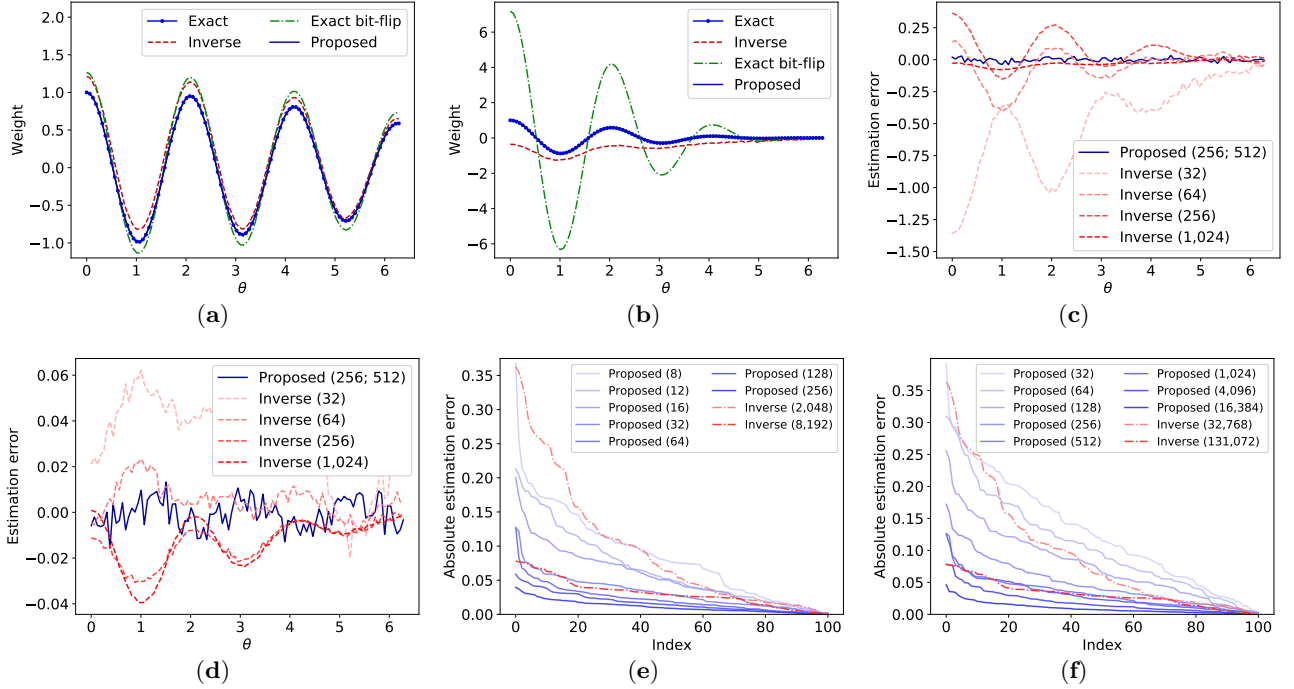


FIG. 4. Simulation results for exact and estimate weights for Pauli-Z operators in a twelve-qubit system with (a) a single σ_z term on the first qubit, and (b) all σ_z terms using 256 random circuits and 512 measurement per circuit for the proposed method and the same total number of measurements for the matrix-inversion approach. We evaluate the method for a range of θ values, resulting in different solutions as given by (14). Plots (c) and (d) give the estimation error for the Pauli operators in (b) and (a), respectively, for easy comparison. The proposed method again uses 256 random circuits with 512 measurements each. For the matrix-inversion approach we sample each of the 2^{12} circuits 32 to 1,024 times. Keeping the number of measurements fixed to 512, plot (e) shows the sorted approximation errors over the θ value, for different numbers of circuits. For the inverse approach we show the equivalent number of circuits such that the product gives the total number of measurements. Plot (f) keeps number of circuits in the proposed approach fixed to 32 and varies the number of measurements per circuit. For the inverse approach we list the equivalent number as before.

VI. CONCLUSIONS

In this work we have proposed an efficient, yet exceedingly simple, method for readout error mitigation in the estimation of Pauli observables. Unlike most existing techniques, the proposed approach does not require any *a priori* assumptions or model of the readout-error

process. The approach is based on the augmentation of quantum circuits with randomly selected Pauli operators and the evaluation of a scalar function based on the measurements obtained using a series of random instances. Readout errors are then mitigated simply by dividing the function value for the quantum circuit of interest by that of the benchmark circuit. The approach

works by diagonalizing the readout-error transfer matrix in the Hadamard domain, which makes it trivial to invert. In contrast to many of the existing algorithms, the proposed approach directly estimates the weight of the Pauli-Z components in the state, rather than the distribution of the distribution of measurement values. Our simulations show that the method is capable of mitigating correlated readout error in a twelve-qubit system with very few measurements and circuit instances.

After completion of the manuscript we became aware of the independent work by Chen *et al.* [38] that contains similar ideas as those presented here.

ACKNOWLEDGMENTS

We thank Sergey Bravyi for helpful comments and discussion. This work is supported by the IBM Research Frontiers Institute.

-
- [1] A. Peruzzo, J. McClean, P. Shadbolt, M.-H. Yung, X.-Q. Zhou, P. J. Love, A. Aspuru-Guzik, and J. L. O’Brien, *Nature communications* **5**, 4213 (2014).
 - [2] P. J. O’Malley, R. Babbush, I. D. Kivlichan, J. Romero, J. R. McClean, R. Barends, J. Kelly, P. Roushan, A. Tranter, N. Ding, *et al.*, *Physical Review X* **6**, 031007 (2016).
 - [3] A. Kandala, A. Mezzacapo, K. Temme, M. Takita, M. Brink, J. M. Chow, and J. M. Gambetta, *Nature* **549**, 242 (2017).
 - [4] R. LaRose, A. Tikku, É. O’Neel-Judy, L. Cincio, and P. J. Coles, *npj Quantum Information* **5**, 1 (2019).
 - [5] V. Havlíček, A. D. Córcoles, K. Temme, A. W. Harrow, A. Kandala, J. M. Chow, and J. M. Gambetta, *Nature* **567**, 209 (2019).
 - [6] M. Schuld and N. Killoran, *Physical review letters* **122**, 040504 (2019).
 - [7] S. McArdle, T. Jones, S. Endo, Y. Li, S. C. Benjamin, and X. Yuan, *npj Quantum Information* **5**, 1 (2019).
 - [8] K. Mitarai, Y. O. Nakagawa, and W. Mizukami, *Physical Review Research* **2**, 013129 (2020).
 - [9] P. W. Shor, *Physical Review A* **52**, R2493 (1995).
 - [10] D. Gottesman, arXiv preprint quant-ph/9705052 (1997).
 - [11] S. J. Devitt, W. J. Munro, and K. Nemoto, *Reports on Progress in Physics* **76**, 076001 (2013).
 - [12] D. A. Lidar and T. A. Brun, *Quantum error correction* (Cambridge university press, 2013).
 - [13] K. Temme, S. Bravyi, and J. M. Gambetta, *Physical review letters* **119**, 180509 (2017).
 - [14] Y. Li and S. C. Benjamin, *Physical Review X* **7**, 021050 (2017).
 - [15] X. Bonet-Monroig, R. Sagastizabal, M. Singh, and T. O’Brien, *Physical Review A* **98**, 062339 (2018).
 - [16] S. Endo, S. C. Benjamin, and Y. Li, *Physical Review X* **8**, 031027 (2018).
 - [17] J. R. McClean, Z. Jiang, N. C. Rubin, R. Babbush, and H. Neven, *Nature Communications* **11**, 1 (2020).
 - [18] S. Endo, Z. Cai, S. C. Benjamin, and X. Yuan, arXiv preprint arXiv:2011.01382 (2020).
 - [19] A. Lowe, M. H. Gordon, P. Czarnik, A. Arrasmith, P. J. Coles, and L. Cincio, arXiv preprint, arXiv:2011.01157 (2020).
 - [20] B. Koczor, arXiv preprint arXiv:2011.05942 (2020).
 - [21] W. J. Huggins, S. McArdle, T. E. O’Brien, J. Lee, N. C. Rubin, S. Boixo, K. B. Whaley, R. Babbush, and J. R. McClean, arXiv preprint arXiv:2011.07064 (2020).
 - [22] A. Kandala, K. Temme, A. D. Córcoles, A. Mezzacapo, J. M. Chow, and J. M. Gambetta, *Nature* **567**, 491 (2019).
 - [23] C. Song, J. Cui, H. Wang, J. Hao, H. Feng, and Y. Li, *Science Advances* **5** (2019).
 - [24] M. Paris and J. Řeháček, eds., *Quantum state estimation*, Vol. 649 (Springer Science & Business Media, 2004).
 - [25] M. R. Geller, *Quantum Science and Technology* **5** (2020).
 - [26] F. B. Maciejewski, Z. Zimborás, and M. Oszmaniec, *Quantum* **4** (2020).
 - [27] E. Haapasalo, T. Heinosaari, and J.-P. Pellonpää, *Quantum Information Processing* **11**, 1751 (2012).
 - [28] M. Steffen, M. Ansmann, R. C. Bialczak, N. Katz, E. Lucero, R. McDermott, M. Neeley, E. M. Weig, A. N. Cleland, and J. M. Martinis, *Science* **313**, 1423 (2006).
 - [29] Y. Chen, M. Farahzad, S. Yoo, and T.-C. Wei, *Physical Review A* **100**, 052315 (2019).
 - [30] B. Nachman, M. Urbaneck, W. A. de Jong, and C. W. Bauer, arXiv preprint arXiv:1910.01969 (2019).
 - [31] K. E. Hamilton, T. Kharazi, T. Morris, A. J. McCaskey, R. S. Bennink, and R. C. Pooser, in *2020 IEEE International Conference on Quantum Computing and Engineering (QCE)* (2020) pp. 430–440.
 - [32] H. Kwon and J. Bae, arXiv preprint arXiv:2003.12314 (2020).
 - [33] S. S. Tannu and M. K. Qureshi, in *Proceedings of the 52nd Annual IEEE/ACM International Symposium on Microarchitecture, MICRO ’52* (Association for Computing Machinery, New York, NY, USA, 2019) p. 279–290.
 - [34] R. Hicks, C. W. Bauer, and B. Nachman, arXiv preprint arXiv:2010.07496 (2020).
 - [35] S. Bravyi, S. Sheldon, A. Kandala, D. C. McKay, and J. M. Gambetta, *Physical Review A* **103**, 042605 (2021).
 - [36] A. Erhard, J. J. Wallman, L. Postler, M. Meth, R. Stricker, E. A. Martinez, P. Schindler, T. Monz, J. Emerson, and R. Blatt, *Nature Communications* **10**, 1 (2019).
 - [37] S. T. Flammia and J. J. Wallman, arXiv preprint arXiv:1907.12976 (2019).
 - [38] S. Chen, W. Yu, P. Zeng, and S. T. Flammia, arXiv preprint arXiv:2011.09636 (2020).